TECHNICAL ARTICLE

Crystal chemistry and X-ray diffraction patterns for $Co(Ni_xZn_{1-x})Nb_4O_{12}$ (x = 0.2, 0.4, 0.6, 0.8)

G. Liu,[1] W. Wong-Ng,[2,a)] and J. A. Kaduk[3,4]
[1]School of Scientific Research, China University of Geosciences, Bejing 100083, People's Republic of China
[2]Materials Measurement Science Division, National Institute of Standards and Technology, Gaithersburg, Maryland 20899
[3]Department of Chemistry, Illinois Institute of Technology, Chicago, Illinois 60616
[4]Department of Physics, North Central College, Naperville, Illinois 60540

(Received 5 July 2016; accepted 6 September 2016)

X-ray reference powder patterns and structures have been determined for a series of cobalt-, nickel- and zinc-containing niobates, $Co(Ni_xZn_{1-x})Nb_4O_{12}$ (x = 0.2, 0.4, 0.6, 0.8). The $Co(Ni_xZn_{1-x})Nb_4O_{12}$ series crystallize in the space group of *Pbcn*, which is of the disordered columbite-type structure (α-PbO_2). The lattice parameters range from a = 14.11190(13) to 14.1569(3) Å, b = 5.69965(6) to 5.71209(13) Å, c = 5.03332(5) to 5.03673(11) Å, and V = 404.844(8) to 407.296(17) Å^3 from x = 0.8 to 0.2, respectively. $Co(Ni_xZn_{1-x})Nb_4O_{12}$ contains double zig-zag chains of NbO_6 octahedra and single chain of $(Ni,Zn,Co)O_6$ octahedra run parallel to the *bc*-plane. Within the same chain the NbO_6 octahedra share edges, while the adjacent NbO_6 chains are joined to each other through common oxygen corners. These double NbO_6 chains are further linked together along the [100]-direction through another $(Co,Ni,Zn)O_6$ units, via common oxygen corners. The edge-sharing $(Co,Ni,Zn)O_6$ also forms zig-zag chains along the *c*-axis. Powder X-ray diffraction patterns of this series of compounds have been submitted to be included in the Powder Diffraction File. © *2016 International Centre for Diffraction Data*. [doi:10.1017/S0885715616000531]

Key words: $Co(Ni_xZn_{1-x})Nb_4O_{12}$, columbite-type structure, powder X-ray diffraction patterns, thermoelectric oxides

I. INTRODUCTION

Columbite compounds possess interesting properties and applications (Pullar, 2009). In the area of wireless communication technologies operating at microwave frequencies, there is an increasing demand for low-cost, high-performance dielectric ceramics. Columbite niobates such as $ZnNb_2O_6$ and $MgNb_2O_6$ have potential applications as microwave materials. Photo-induced splitting of water to produce H_2 is very important because of environmental, energy, and sustainability concerns; the catalytic properties of columbites are demonstrated by the photoelectrochemical behavior of reduced $NiNb_2O_6$ single-crystal electrodes (Guochang *et al*., 1991). Columbites also have unusual optical and magnetic properties (Senegas & Galy 1972). Two kinds of luminescence have been investigated so far, rare-earth activated emission (laser applications) and self-activated emission in pure columbites. Rare-earth-doped luminescence materials such as Er^{3+}: $CdNb_2O_6$ are attractive because of their thermal and chemical stabilities (Erdem *et al.*, 2014; Wong-Ng *et al.*, 1987). $CaNb_2O_6$ is a self-activated blue phosphor. Columbite niobates such as $FeNb_2O_6$, $NiNb_2O_6$, and $MnNb_2O_6$ exhibit magnetic ordering at rather low temperature, with a Néel temperature (TN) of 3–6 K (Hanawa *et al.*, 1994; Huang *et al.*, 2014).

Another possible area of application for columbites is energy conversion, for example, waste heat conversion into electricity. Despite significant efforts in searching for efficient oxides (stability at high temperatures) for energy conversion, the material performance at high temperature still needs a significant improvement. As cobaltate compounds, including $NaCoO_x$ (Terasaki, *et al.*, 1997; $Ca_2Co_3O_6$ (Mikami *et al.*, 2003; Mikami & Funahashi, 2005), $Ca_3Co_4O_9$ (Masset *et al.*, 2000; Minami, *et al.*, 2002; Grebille *et al.*, 2004; Wong-Ng *et al.*, 2007), and $Bi_2Sr_2Co_2O_x$ (Wang *et al.*, 2009) have shown promising thermoelectric properties, the search for low-dimensional compounds such as two-dimensional (2D)-layered and 1D-chain cobaltate compounds with improved thermoelectric properties continues in our laboratory, including phase diagram studies of ternary oxide systems, including CaO and Co_3O_4 as two of the end members (Wong-Ng *et al.*, 2010, 2011, 2013, 2014).

A detailed study of the effects of non-stoichiometry of $(Zn, Co)Nb_2O_6$ and $(Ni, Zn)Nb_2O_6$ have been reported by Belous *et al.* (2007) and Butee *et al.* (2009), respectively. In this paper, we are interested in the solid solution formation of the $(Co,Zn,Ni)Nb_4O_{12}$ columbite compounds. The first goal of this paper is to investigate the structure of the Co $(Ni_xZn_{1-x})Nb_4O_{12}$ (x = 0.2, 0.4, 0.6, 0.8) series, in particular, the effect of the larger size of Zn^{2+} (Shannon, 1976) on substituting on the Ni site. In these compositions, the concentration of Co^{2+} was kept constant. Since X-ray diffraction (XRD) is a non-destructive technique for phase identification, XRD patterns are especially important for phase characterization; therefore the second goal of this paper is to determine the experimental patterns for $Co(Ni_xZn_{1-x})Nb_4O_{12}$ (x = 0.2, 0.4, 0.6, 0.8), and to make them available through submission to the Powder Diffraction File (PDF) (2016).

a)Author to whom correspondence should be addressed. Electronic mail: winnie.wong-ng@nist.gov

II. EXPERIMENTAL

A. Sample preparation

Samples were prepared from stoichiometric amounts of NiO, ZnO, Co_3O_4, and Nb_2O_5 using solid-state high-temperature techniques. The starting samples were mixed, pelletized, and heat treated in air at 800 °C for 12 h and subsequently annealed at 1100 °C for 12 h, 1300 °C for 24 h with intermediate grindings. During each heat treatment in air, the samples were furnace cooled. The heat treatment process was repeated until no further changes were detected in the powder XRD patterns.

B. X-ray Rietveld refinements and powder reference patterns

The $Co(Ni_xZn_{1-x})Nb_4O_{12}$ series ($x = 0.2$, 0.4, 0.6, 0.8) powders were mounted as ethanol slurries on zero-background cells. The X-ray powder patterns were measured (5° to 130° 2θ, 0.0202144° steps, 0.5 s step^{-1}, CuK_α radiation) on a Bruker D2 Phaser diffractometer equipped with a LynxEye detector. (The purpose of identifying the equipment in this paper is to specify the experimental procedure. Such identification does not imply recommendation or endorsement by the National Institute of Standards and Technology.) To reduce effects of fluorescence, the lower limit of the multichannel analyzer was changed from its default value of 0.11–0.19 V.

The Rietveld refinement technique (Rietveld, 1969) with the software suite GSAS (Larson and Von Dreele, 2004) was used to determine the structure of the $Co(Ni_xZn_{1-x})Nb_4O_{12}$ series ($x = 0.2$, 0.4, 0.6, 0.8) compounds. The structure of $Nb_2Fe_{0.4}Co_{0.6}O_6$ (Sarvezuk *et al.*, 2011) was used as the starting model for the refinements. Reference patterns were obtained using a Rietveld pattern decomposition technique. Using this technique, the reported peak intensities were derived from the extracted integrated intensities, and positions calculated from the lattice parameters. The pseudo-Voigt function (profile function #4) was used for the refinement of both series of compounds (Thompson *et al.*, 1987; Finger *et al.*, 1994; Stephens, 1999). When peaks are not resolved at the resolution function, the intensities are summed, and an intensity-weighted *d*-spacing is reported. In summary, these patterns represent ideal specimen patterns.

C. Bond-valence sum (BVS) calculations

The *BVS* values for Ni, Zn, Nb, and Co sites were calculated using the Brown–Altermatt empirical expression (Brown and Altermatt, 1985; Brese and O'Keeffe, 1991). The *BVS* of an atom *i* is defined as the sum of the bond valences v_{ij} of all the bonds from atoms *i* to *j*. The most commonly adopted empirical expression for the bond valence v_{ij} as a function of the interatomic distance d_{ij} is $v_{ij} = \exp[(R_0 - d_{ij})/B]$. The parameter, *B*, is commonly taken to be a "universal" constant equal to 0.37 Å. The values for the reference distance R_0 for Ni^{2+}–O, Zn^{2+}–O, Co^{2+}–O, and Nb^{5+}–O, are 1.654, 1.704, 1.692, and 1.911, respectively (Brown and Altermatt, 1985; Brese and O'Keeffe, 1991). In the sites where there are more than two different types of atoms, the BVS value is the weighted sum of the fraction of occupancy.

TABLE I. Rietveld refinement residuals (R_{wp}, R_p, and χ^2) (Larson and Von Dreele, 2004) for $Co(Ni_xZn_{1-x})Nb_4O_{12}$.

x	R_{wp}	R_p	χ^2
0.2	0.0400	0.0305	1.18
0.4	0.0557	0.0404	1.58
0.6	0.0311	0.0414	1.26
0.8	0.0435	0.0317	1.31

III. RESULTS AND DISCUSSION

Table 1 gives the Rietveld refinement results for the $Co(Ni_xZn_{1-x})Nb_4O_{12}$ compounds. The pseudo-Voight function profile function #2 with 18 terms was used for the refinements (Howard, 1982; Thompson *et al.*, 1987). Figure 1 provides the Rietveld refinement results for $Co(Ni_{0.4}Zn_{0.6})Nb_4O_{12}$ as an example. The observed (crosses), calculated (solid line), and difference XRD patterns (bottom) are shown. The difference pattern is plotted at the same scale as the other patterns up to 70° 2θ. At higher angles, the scale has been magnified five times. An excellent agreement between observed and calculated profiles is demonstrated.

Table 2 provides the crystallographic data for $Co(Ni_{0.4}Zn_{0.6})Nb_4O_{12}$ (the number inside the bracket refers to standard deviation). The $Co(Ni_xZn_{1-x})Nb_4O_{12}$ series crystallizes in the orthorhombic space group *Pbcn*, and its structure is essentially of a disordered columbite-type structure (α-PbO_2) (Filatov *et al.*, 2005). The lattice parameters of the series range from $a = 14.11190(13)$ to 14.1569(3) Å, $b =$ 5.69965(6) to 5.71209(13) Å, $c = 5.03332(5)$ to 5.03673 (11) Å, and $V = 404.844$ (8) to 407.30 (2) Å^3 for $x = 0.8$ to 0.2. As the ionic radius of Zn^{2+} is smaller than that of Ni^{2+} (Shannon, 1976), a monotonic decreasing trend of unit-cell volume (as a function of x) is observed in Figure 2. The atomic coordinates and displacement parameters are listed in Table 3.

The structure of the $Co(Ni_{0.4}Zn_{0.6})Nb_4O_{12}$ solid solution was confirmed to be of the distorted columbite type (Sturdivant, 1930; Bordet *et al.*, 1986; Pagola and Carbonio,

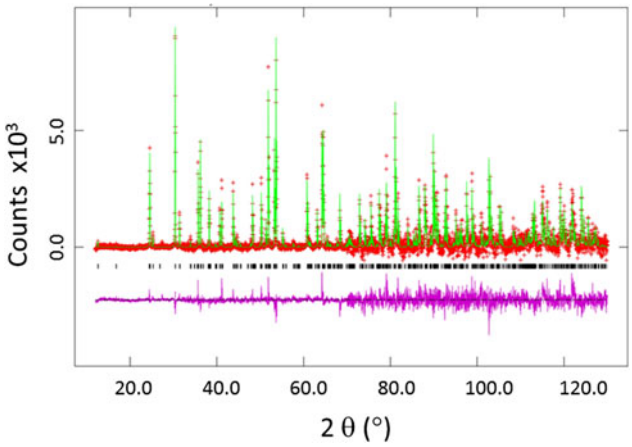

Figure 1. (Colour online) Rietveld pattern for $Co(Ni_{0.4}Zn_{0.6})Nb_4O_{12}$. The observed (crosses), calculated (solid line), and difference XRD patterns (bottom) are shown. The difference pattern is plotted at the same scale as the other patterns up to 70° 2θ. At higher angles, the scale has been magnified five times.

https://doi.org/10.1017/S0885715616000531 Published online by Cambridge University Press

TABLE II. Experimental cell parameters for $Co(Ni_xZn_{1-x})Nb_4O_{12}$ [*Pbcn* (*No. 60*), $Z = 2$]. Numbers inside the brackets represent standard deviation, which resides in the last digit.

Value of "*x*"	*a*	*b*	*c*	*V*
0.2	14.1569 (3)	5.71209 (13)	5.03673 (11)	407.30 (2)
0.4	14.1437 (3)	5.70857 (11)	5.03537 (11)	406.56 (2)
0.6	14.12851 (13)	5.70393 (5)	5.03468 (5)	405.735 (7)
0.8	14.11190 (13)	5.69965 (6)	5.03332 (5)	404.844 (8)

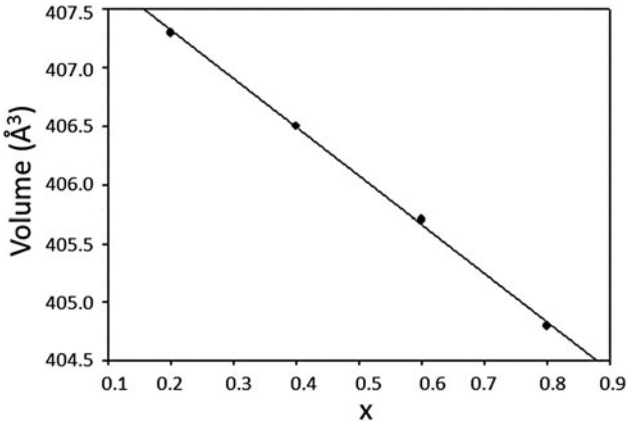

Figure 2. Plot of unit-cell volume, *V*, of $Co(Ni_xZn_{1-x})Nb_4O_{12}$ as a function of *x*. A monotonic trend of decrease of *V* as a function of *x* is observed. The line is a guide for the eyes.

1997; Pullar, 2009). Figures 3–5 give the crystal structure with views projected along *a*-, *b*-, and *c*-axes, respectively. The structure, in general, contains double zig-zag chains of NbO_6 octahedra and edge-sharing $(Co,Ni,Zn)O_6$ octahedra running parallel to the *bc*-plane (Fig. 3). Within the same chain the NbO_6 octahedra share edges via O5 and O7, while the adjacent NbO_6 chains are joined to each other through common corners, O7 (Fig. 4). These double NbO_6 chains are further linked together along the [100]-direction through another $(Co,Ni,Zn)O_6$ units, via O5 and O6 in common corners (Fig. 5).

Both the NbO_6 and $(Co,Ni,Zn)O_6$ octahedra are distorted. The distorted Nb and (Co,Ni,Zn) sites are evidenced from the different octahedral Nb–O distances and the (Co,Ni,Zn)–O distances. For example, the Nb–O distances range from 1.977(6) to 2.140(5) Å, and the (Co,Ni,Zn)–O distances range from 1.960(5) to 2.008(5) Å, respectively. Similarly, the octahedral bond angles were also found to be deviated from the ideal 90°. The most distorted angles in these four members range from 67.2(4)° to 75.4(5)° in NbO_6 and 76.5 (3)° to 77.9(3)° in $(Co,Ni,Zn)O_6$.

The BVS values in $Co(Ni_xZn_{1-x})Nb_4O_{12}$ show a large compressive stress at the (Ni/Zn/Co) sites and a large tensile stress for the Nb sites for all four compositions. From $x =$ 0.2 to 0.8, the "ideal BVS" values are 2.0 and 5.0 for the (Ni/Zn/Co) and Nb sites, respectively. The experimental BVS were found to range from 3.91 to 4.06 along the

TABLE III. Atomic coordinates and displacement factors for compounds for $Co(Ni_xZn_{1-x})Nb_4O_{12}$ [*Pbcn* (*No. 60*), $Z = 2$]; M represents site symmetry multiplicity; WS represents Wyckoff symbol. The coordinate values pertaining to the oxygen atoms were not refined during the refinement process. Numbers inside the brackets represent standard deviation, which resides in the last digit.

Atom	*x*	*y*	*z*	Site **O**cc.	U_{iso}	WS
(1) $Co(Ni_{0.2}Zn_{0.8})Nb_4O_{12}$						
Ni1/Zn2/Co3	0.0	0.1634 (11)	0.25	0.1/0.4/0.5	0.016 (2)	4*c*
Nb4	0.1599 (2)	0.3161 (4)	0.744 (2)	1.0	0.0175 (8)	8*d*
O5	0.0922 (7)	0.3850 (15)	0.395 (2)	1.0	0.040 (2)	8*d*
O6	0.0773 (5)	0.0823 (14)	0.9348 (14)	1.0	0.040 (2)	8*d*
O7	0.2638 (8)	0.108 (2)	0.586 (3)	1.0	0.040 (2)	8*d*
(2) $Co(Ni_{0.4}Zn_{0.6})Nb_4O_{12}$						
Ni1/Zn2/Co3	0.0	0.1575 (15)	0.25	0.2/0.3/0.5	0.032 (3)	4*c*
Nb4	0.1603 (3)	0.3195 (5)	0.745 (2)	1.0	0.0087 (7)	8*d*
O5	0.1033 (10)	0.364 (2)	0.375 (3)	1.0	0.039 (4)	8*d*
O6	0.0768 (7)	0.087 (2)	0.932 (2)	1.0	0.039 (4)	8*d*
O7	0.2659 (10)	0.110 (2)	0.591 (3)	1.0	0.039 (4)	8*d*
(3) $Co(Ni_{0.6}Zn_{0.4})Nb_4O_{12}$						
Ni1/Zn2/Co3	0.0	0.1596 (10)	0.25	0.3/0.2/0.5	0.019 (2)	4*c*
Nb4	0.1598 (2)	0.3188 (3)	0.746 (2)	1.0	0.0113 (5)	8*d*
O5	0.1037 (6)	0.3620 (14)	0.374 (2)	1.0	0.002 (2)	8*d*
O6	0.0721 (6)	0.0979 (14)	0.9217 (13)	1.0	0.002 (2)	8*d*
O7	0.2654 (7)	0.1127 (15)	0.594 (2)	1.0	0.002 (2)	8*d*
(4) $Co(Ni_{0.8}Zn_{0.2})Nb_4O_{12}$						
Ni1/Zn2/Co3	0.0	0.1562 (11)	0.25	0.4/0.1/0.5	0.033 (2)	4*c*
Nb4	0.1596 (2)	0.3184 (3)	0.747 (2)	1.0	0.0171 (6)	8*d*
O5	0.0938 (8)	0.3810 (16)	0.399 (2)	1.0	0.027 (2)	8*d*
O6	0.0763 (6)	0.0913 (15)	0.9312 (14)	1.0	0.027 (2)	8*d*
O7	0.2624 (8)	0.1038 (17)	0.581 (3)	1.0	0.027 (2)	8*d*

https://doi.org/10.1017/S0885715616000531 Published online by Cambridge University Press

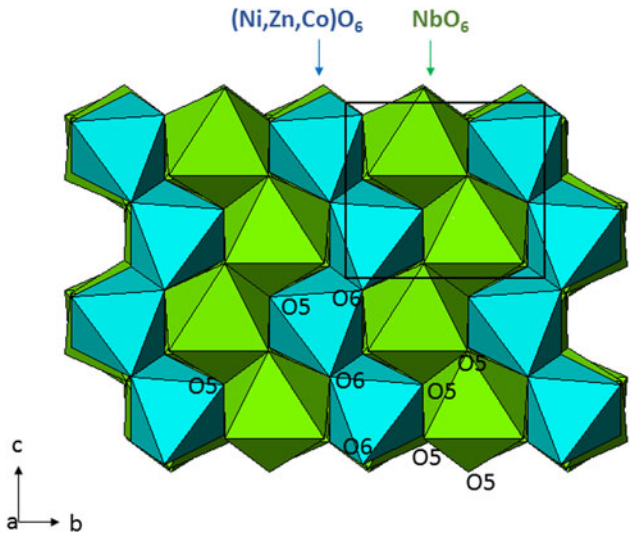

Figure 3. (Colour online) View of the crystal structure of $Co(Ni_xZn_{1-x})Nb_4O_{12}$ along the *a*-axis. The structure consists of zig-zag chains of NbO_6 and $(Ni,Zn,Co)O_6$ octahedral units along the *c*-axis.

Nb-site from $x = 0.2$ to 0.8, indicating tensile stress, as these values are much smaller than "5" (or the cage at which Nb resides is too large). On the other hand, the BVS value for the mixed (Ni/Zn/Co) site ranges from 2.75 down to 2.66 as the

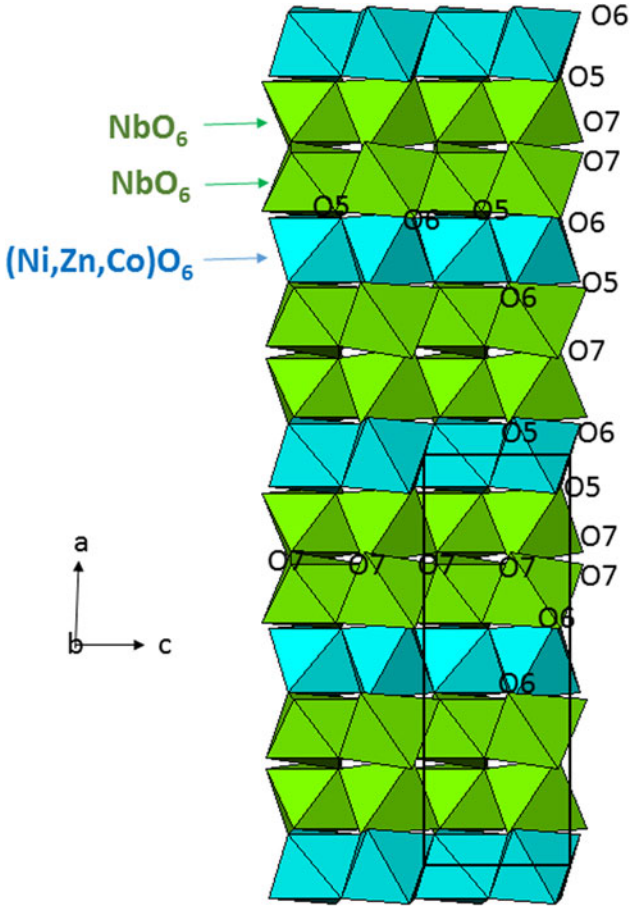

Figure 4. (Colour online) View of the crystal structure of $Co(Ni_xZn_{1-x})Nb_4O_{12}$ along the *b*-axis. Double chains of NbO_6 and single chain of $(Ni,Zn,Co)O_6$ octahedra run parallel along the *c*-axis.

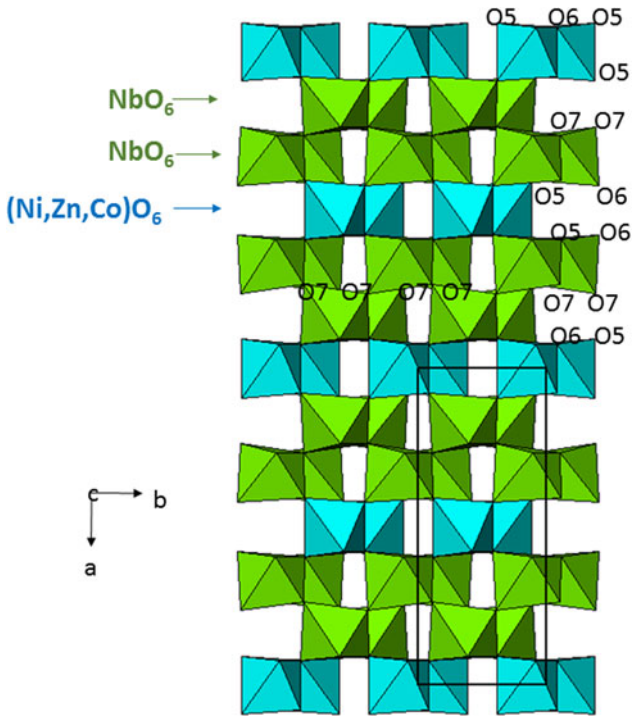

Figure 5. (Colour online) View of the crystal structure of $Co(Ni_xZn_{1-x})Nb_4O_{12}$ along the *c*-axis. Double chains of NbO_6 and single chain of $(Ni,Zn,Co)O_6$ octahedra run parallel to the *bc*-plane.

x-value decreases, representing substantial compressive stress, even though the value decreases somewhat as the amount of the larger Ni^{2+} increases (Table 4).

A. Reference XRD patterns

An example of reference patterns of, $Co(Ni_{0.4}Zn_{0.6})Nb_4O_{12}$, is given in Table 5. In these patterns, the symbol "M" refers to peaks containing contributions of two reflections. The particular peak that has the strongest intensity in the entire pattern is assigned an intensity of 999 and other lines are scaled relative to this value. In general, the *d*-spacing values are calculated values from refined lattice parameters. The intensity values reported are integrated intensities (rather than peak heights) based on the corresponding profile parameters as reported in Table 5. For resolved overlapped peaks, intensity-weighted calculated *d*-spacing, along with the observed integrated intensity and the *hkl* indices of both peaks (for "M") are used. For peaks that are not resolved at the instrumental resolution, the intensity-weighted average *d*-spacing and the summed integrated intensity value are used. In the case of a cluster, unconstrained profile fits often reveal the presence of multiple peaks, even when they are closer than the instrumental resolution. In this situation, both *d*-spacing and intensity values are reported independently. All patterns of $Co(Ni_xZn_{1-x})Nb_4O_{12}$ ($x = 0.2$, 0.4, 0.6, 0.8) have been submitted for inclusion in the PDF.

B. Summary

The end members $(Co,Ni)Nb_2O_6$ and $(Co,Zn)Nb_2O_6$ form a complete solid solution $Co(Ni_xZn_{1-x})Nb_4O_{12}$. The X-ray

https://doi.org/10.1017/S0885715616000531 Published online by Cambridge University Press

TABLE IV. Bond distances and BVS values for $Co(Ni_xZn_{1-x})Nb_4O_{12}$ [*Pbcn* (*No. 60*), $Z = 2$]. In the sites where there are more than two different types of atoms, the BVS is the weighted sum of the fraction of occupancy. The ideal BVS values for (Ni1/Zn2/Co3) and Nb sites are 2.0 and 5.0 respectively for all four compositions. Numbers inside the brackets represent standard deviation, which resides in the last digit.

Atom	Atom	Distances (Å)							
		(i) $x = 0.2$	BVS	(ii) $x = 0.4$	BVS	(iii) $x = 0.6$	BVS	(iv) $x = 0.8$	BVS
Ni1/Zn2/Co3	O5 × 2	1.960 (5)	2.74	1.981 (6)	2.75	1.967 (5)	2.73	1.989 (5)	2.66
	O6 × 2	1.983 (5)		1.979 (6)	1.973 (5)	1.968 (5)			
	O6 × 2	2.008 (5)		1.989 (6)	1.985 (5)	1.996 (5)			
Nb4	O5	2.040 (6)	3.91	2.044 (8)	3.98	2.049 (6)	4.03	2.012 (7)	4.06
	O5	2.100 (6)		2.084 (8)		2.088 (6)		2.094 (6)	
	O6	2.017 (6)		2.012 (8)		1.977 (6)		1.980 (6)	
	O7	2.052 (5)		2.066 (7)		2.048 (6)		2.074 (6)	
	O7	2.140 (5)		2.105 (8)		2.124 (6)		2.134 (7)	
	O7	2.079 (6)		2.071 (8)		2.083 (6)		2.058 (7)	

TABLE V. X-ray powder pattern for $Co(Ni_{0.4}Zn_{0.6})Nb_4O_{12}$ [*Pbcn* (*No. 60*), $Z = 2$]. $a = 14.1437$ (3) Å, $b = 5.70857(11)$ Å, $c = 5.03537(11)$ Å, $V = 406.56(2)$ Å^3, and $Z = 2$. The symbols "M" refers to peaks containing contributions from two reflections. The particular peak that has the strongest intensity in the entire pattern is assigned an intensity of 999 and other lines are scaled relative to this value. The *d*-spacing values are calculated values from refined lattice parameters, and "I_{obs}" represents integrated intensity values.

d_{cal}	I_{obs}	h	k	l	d_{cal}	I_{obs}	h	k	l	d_{cal}	I_{obs}	h	k	l
7.0719	30	2	0	0	5.2937	24	1	1	0	3.6484	43	1	1	1
3.6351	383	3	1	0	3.5359	89	4	0	0	2.9474	999	3	1	1
2.8543	105	0	2	0	2.5177	127	0	0	2	2.4831	172	0	2	1
2.3573	114	6	0	0	2.2209	43	4	2	0M	2.2209	43	3	0	2M
2.1970	67	3	2	1	2.0697	83	3	1	2	2.0509	18	4	0	2
2.0321	14	4	2	1	1.9301	10	4	1	2	1.9047	8	7	1	0
1.8878	85	0	2	2M	1.8878	85	1	3	0M	1.8176	79	6	2	0
1.7815	39	7	1	1	1.7646	174	3	3	0	1.7208	156	6	0	2
1.7096	253	6	2	1	1.6654	41	4	2	2M	1.6654	4	3	3	1M
1.6000	17	1	1	3	1.5239	164	3	1	3	1.5152	13	9	1	0
1.5094	8	1	3	2	1.4737	67	6	2	2	1.4509	171	9	1	1
1.4468	63	0	2	3	1.4450	130	3	3	2	1.4271	7	0	4	0
1.4144	11	10	0	0	1.3853	18	7	3	0	1.3731	61	0	4	1
1.3279	7	9	2	1	1.2982	28	9	1	2	1.2800	11	4	4	1
1.2593	12	7	1	3	1.2588	13	0	0	4	1.2331	33	10	0	2M
1.2331	33	6	2	3M	1.2290	16	10	2	1	1.2137	15	7	3	2
1.2117	34	9	3	0	1.2006	4	3	4	2	1.1895	11	3	1	4
1.1865	72	6	4	1	1.1786	38	12	0	0	1.1518	23	0	2	4
1.1320	7	10	2	2	1.1247	42	9	1	3	1.1104	32	6	0	4
1.1096	16	3	5	0	1.0985	9	6	4	2	1.0952	5	4	2	4
1.0918	60	9	3	2	1.0894	10	12	2	0	1.0873	23	0	4	3
1.0836	26	3	5	1	1.0746	5	2	4	3	1.0675	22	12	0	2
1.0648	35	12	2	1	1.0455	21	13	1	1	1.0392	9	4	4	3
1.0370	5	1	5	2	1.0349	18	6	2	4	1.0248	46	3	3	4
1.0154	25	3	5	2	1.0114	6	10	2	3	0.9998	17	12	2	2
0.9940	6	7	5	0	0.9873	45	6	4	3	0.9852	16	10	4	1
0.9752	4	7	5	1	0.9705	84	3	1	5	0.9683	23	9	1	4
0.9514	5	0	6	0	0.9497	12	0	2	5	0.9445	7	13	3	0
0.9403	5	10	0	4	0.9349	5	0	6	1	0.9316	9	7	3	4
0.9303	7	15	1	0	0.9256	16	3	5	3	0.9246	9	7	5	2
0.9237	14	9	5	0	0.9172	5	4	2	5	0.9148	37	15	1	1
0.9138	39	12	2	3	0.9085	21	9	5	1	0.9015	14	13	1	3
0.8943	61	12	4	1	0.8931	10	10	2	4	0.8900	22	0	6	2
0.8842	29	13	3	2M	0.8842	29	16	0	0M	0.8823	23	6	6	0
0.8809	31	6	2	5	0.8730	44	9	3	4	0.8672	26	9	5	2
0.8620	20	10	4	3	0.8604	24	12	0	4					

patterns and structure of $Co(Ni_xZn_{1-x})Nb_4O_{12}$ ($x = 0.2, 0.4, 0.6, 0.8$) have been determined. $Co(Ni_xZn_{1-x})Nb_4O_{12}$ adopts the columbite structure, which consists of mixed distorted octahedral (Co, Ni, Zn)O_6 and distorted NbO_6 sites. The (Co, Ni, Zn)O_6 sites are under compressive stress, whereas the NbO_6 sites are under tensile stress. Powder X-ray patterns of these four solid solution members have been submitted for inclusion in the PDF.

ACKNOWLEDGEMENT

Partial financial support from ICDD is acknowledged.

SUPPLEMENTARY MATERIAL

The supplementary material for this article can be found at http://dx.doi.org/10.1017/S0885715616000531.

Belous, S., Ovchar, O., Jancar, B., and Bezjak, J. (**2007**). "The effect of non-stoichiometry on the microstructure and microwave dielectric properties of the columbites $A^{2+}Nb^{2}O^{6}$," J. Eur. Ceram. Soc. **27**, 2933–2936.

Bordet, P., McHale, A., Santoro, A., and Roth, R. S. (**1986**). "Powder neutron diffraction study of $ZrTiO_4$, $Zr_5Ti_4O_{24}$, and $FeNb_2O_6$," J. Solid State Chem. **64**, 30–46.

Brese, N. E. and O'Keeffe, M. (**1991**). "Bond-valence parameters for solids," Acta Crystallogr. B **47**, 192–197.

Brown, I. D. and Altermatt, D. (**1985**). "Bond-valence parameters obtained from a systematic analysis of the inorganic crystal structure database," Acta Crystallogr. B **41**, 244–247.

Butee, S., Kulkarni, A., Prakash, O., Aiyar, R. P. R. C., George, S., and Sebatian, M. T. (**2009**). "High Q microwave dielectric ceramics in $(Ni_{1-x}Zn_x)Nb_2O_6$ system," J. Am. Ceram. Soc. **92**, 1047–1053.

Erdem, M., Ghafouri, S., Ekmekçi, M. K., Mergen, A., and Özen, G. (**2014**). "Structural and Spectroscopic Properties of Er3+: CdNb2O6 Phosphors," in *Nano-Structures for Optics and Photonics, NATO Science for Peace and Security Series B: Physics and Biophysics*, edited by Di Bartolo, B. *et al*. (Springer Science and Business Media Dordrecht, Netherlands) 2015, pp. 443–445.

Filatov, S., Bendeliani, N., Albert, B., Kopf, J., Dyuzeva, T., and Lityagina, L. (**2005**). "High-pressure synthesis of α-PbO_2 and its crystal structure at 293, 203, and 113 K from single crystal diffraction data," Solid State Sci. **7**, 1363–1368.

Finger, L. W., Cox, D. E., and Jephcoat, A. P. (**1994**). "A correction for powder diffraction peak asymmetry due to axial divergence," J. Appl. Crystallogr. **27**, 892–900.

Grebille, D., Lambert, S., Bouree, F., and Petricek, V. (**2004**). "Contribution of powder diffraction for structure refinements of aperiodic misfit cobalt oxides," J. Appl. Crystallogr. **37**, 823–831.

Guochang, L., Peeraldo Bicelli, L., and Razzini, G. (**1991**). "Photoelectrochemical characterization of $NiNb_2O_6$," Solar Energy Mater. **21**, 335–346.

Hanawa, T., Shinkawa, K., Ishikawa, M., Miyatani, K., Saito, K., and Kohn, K. (**1994**). "Anisotropic specific heat of $CoNb_2O_6$," Phys. Rev. Jpn. **63**, 2706–2715.

Howard, C. J. (**1982**). "The approximation of asymmetric neutron powder diffraction peaks by sums of Gaussians," J. Appl. Crystallogr. **15**(6), 615–620.

Huang, F., Zhou, Q., Li, L., Huang, X., Xu, D., Li, F., and Cui, T. (**2014**). "Structural transition of $MnNb_2O_6$ under quasi-hydrostatic pressure," J. Phys. Chem. **118**, 19280–19286.

Larson, A. C. and Von Dreele, R. B. (**2004**). *General Structure Analysis System* (GSAS) (Los Alamos National Laboratory Report LAUR 86–748, Los Alamos).

Masset, A. C., Michel, C., Maignan, A., Hervieu, M., Toulemonde, O., Studer, F., Raveau, B., and Hejtmanck, J. (**2000**). "Misfit-layered cobaltite with an anisotropic giant Magnetoresistance: $Ca_3Co_4O_9$," Phys. Rev. B **62**, 166–175.

Mikami, M. and Funahashi, R. (**2005**). "The effect of element substitution on high-temperature thermoelectric properties of $Ca_3Co_2O_6$ compounds", J. Solid State Chem. **178**, 1670–1674.

Mikami, M., Funahashi, R., Yoshimura, M., Mori, Y., and Sasaki, T. (**2003**). "High-temperature thermoelectric properties of single-crystal $Ca_3Co_2O_6$," J. Appl. Phys. **94**(10), 6579–6582.

Minami, H., Itaka, K., Kawaji, H., Wang, Q. J., Koinuma, H. and Lippmaa, M. (**2002**). "Rapid synthesis and characterization of $(Ca_{1-x}Ba_x)_3Co_4O_9$ thin films using combinatorial methods," Appl. Surface Sci. **197**, 442–447.

Pagola, S., Carbonio, R. E. (**1997**). "Crystal structure refinement of $MgNb_2O_6$ columbite from neutron powder diffraction data and study of the ternary powder diffraction data and study of the ternary system MgO-Nb_2O_5–NbO, with evidence of formation of new reduced pseudobrookite $Mg_{5-x}Nb_{4+x}O_{15-\delta}$ ($1.14 \leq x \leq 1.60$) Phases," J. Solid State Chem. **134**, 76–84.

PDF, Powder Diffraction File (**2016**). *Produced by International Centre for Diffraction Data* (12 Campus Blvd., Newtown Square, PA, 19073–3273).

Pullar, R. C. (**2009**). "The synthesis, properties, and applications of columbite niobates ($M^{2+}Nb_2O_6$): a critical review," J. Am. Ceram. Soc., **92**(3), 563–577.

Rietveld, H. M. (**1969**). "A profile refinement method for nuclear and magnetic structures," J. Appl. Crystallogr. **2**, 65–71.

Sarvezuk, P. W. C., Kinast, E. J., Colin, C. V., Cusmäo, M. A., da Cunha, J. B. M., and Isnard, O. (**2011**). "New investigation of the magnetic structure of $CoNb_2O_6$ columbite," J. Appl. Phys. **109**, 07E160.

Senegas, J., Galy, J. (**1972**). "Sur les transformations des structures columbite el trirutilke étude du système $NiNb_2O_6$-NiF," J solid State Chem. **5**, 481–486.

Shannon, R. D. (**1976**). "Revised effective ionic radii and systematic studies of interatomic distances in halides and chaleogenides," Acta Crystallogr. **A32**, 751–767.

Stephens, P. W. (**1999**). "Phenomenological model of anisotropic peak broadening," J. Appl. Crystallogr., **32**, 281–289.

Sturdivant, J. H. (**1930**). "The crystal structure of columbite," Z. Kristallogr. **75**, 66–105.

Terasaki, I., Sasago, Y., Uchinokura, K. (**1997**). "Large thermoelectric power in $NaCo_2O_4$ single crystals," Phys. Rev. B **56**, 12685–12687.

Thompson, P., Cox, D. E. & Hastings, J. B. (**1987**). "Rietveld refinement of Debye–Scherrer synchrotron X-ray data from Al_2O_3", J. Appl. Crystallogr. **20**, 79–83.

Wang, S., Venimadhav, A., Guo, S., Chen, K., Li, Q., Soukiassian, A., Schlom, D. G., Katz, M. B., Pan, X. Q., Wong-Ng, W., Vaudin, M. D., and Xi, X. X. (**2009**). "Structural and thermoelectric properties of $Bi_2Sr_2Co_2O_y$ thin films on $LaAlO_3$ (100) and fused silica substrates," Appl. Phys. Lett. **94**, 022110.

Wong-Ng, W., McMurdie, H. F., Paretzkin, B., and Zhang, Y., Davis, K. L., Hubbard, C. R., Dragoo, A. L., and Stewart, J. M. (**1987**). "Standard X-ray diffraction powder patterns of sixteen ceramic phases," Powder Diffr. **2** (3), 191–202.

Wong-Ng, W., Hu, Y. F., Vaudin, M. D., He, B., Otani, M., Lowhorn, N. D., and Li, Q. (**2007**). "Texture and phase analysis of a $Ca_3Co_4O_9$ thermoelectric film on Si (100) substrate," J. Appl. Phys. **102**(3), 33520.

Wong-Ng, W., Liu, G., Martin, J., Thomas, E. L., Lowhorn, N., and Kaduk, J. A. (**2010**). "Phase compatibility of the thermoelectric properties of compounds in the Sr–Ca–Co–O system," J. Appl. Phys. **107**, 033508.

Wong-Ng, W., Luo, T., Xie, W., Tang, W. H., Kaduk, J. A., Huang, Q., Yan, Y., Tang, X., and Tritt, T. (**2011**). "Phase diagram, crystal chemistry and thermoelectric properties of compounds in the Ca–Co–Zn–O system," J. Solid State Chem. **184**(8), 2159–2166.

Wong-Ng, W., Laws, W. J., Yan, Y. G. (**2013**). "Phase diagram and crystal chemistry of the La–Ca–Co–O system", Solid State Sci. **17**, 107–110.

Wong-Ng, W., Laws, W. J., Talley, K. R., Huang, Q., Yan, Y., Martin, J., and Kaduk, J. A. (**2014**). "Phase equilibria and crystal chemistry of the CaO–$\frac{1}{2}Nd_2O_3$–CoO_z system at 885 °C in air," J. Solid State Chem. **215**, 128–134.